

Authigenic siliceous-carbonate concretions in Cenomanian–Turonian carbonates of southern Croatia; geochemical and biotic record

Hrvoje Posilović¹ · Karmen Fio Firi² · Jasenka Sremac² · Blanka Cvetko Tešović² · Marija Brajković³

Received: 9 December 2015 / Accepted: 26 August 2016 / Published online: 8 September 2016
© Springer-Verlag Berlin Heidelberg 2016

Abstract Numerous regular and irregularly shaped concretions were discovered in southern Croatia within the Upper Cretaceous carbonate deposits, which consist mostly of bioclastic wackestones and packstones. The size of the concretions varies from 2 to 25 cm in diameter for the regular, and up to 40 cm in length for the irregular ones. The concretions have different internal structures and compositions, which vary from those of the host rocks. Some concretions are entirely siliceous, while others exhibit alternating opal silica and carbonate-rich zones. Silica is derived from opal-A secreting marine biota, mostly sponges, whose spicules can be found within the concretions and in the surrounding limestones. The regular shape and alterations of zones are the result of the diffusive supply and fast “consummation” of silica at the growth site. Determined fossil community and bitumen found in the surrounding limestones indicate deposition in the oxygen-depleted deep-marine environment of the Adriatic Carbonate Platform, which belongs to the Sveti Duh Formation (latest Cenomanian–Early Turonian). The carbon isotope composition of the concretions corresponds to the globally known Cenomanian–Turonian ‘Oceanic Anoxic Event’ (OAE 2).

Keywords Concretions · Silica-carbonate · Diffusion · Late Cretaceous · Oceanic Anoxic Event · Southern Croatia

Introduction

During road excavations in southern Croatia (Pojezerje municipality; Fig. 1a), numerous regularly shaped spherical concretions were released from the parent limestones. Field investigation, together with micropaleontological, petrological, and geochemical analyses, provided different lines of evidence used to interpret the formation and alteration processes, and timing of this peculiar phenomenon.

According to Bates and Jackson (1987; in Macsotay et al. 2003), a concretion is a hard compact mass or aggregate of mineral matter, normally subspherical, but commonly oblate, disk-shaped, or irregular with odd or fantastic outlines. Concretions are formed by precipitation from aqueous solution around a nucleus, such as leaf, shell, bone, or fossil, and usually of a composition widely different from that of the rock in which it is found and from which it is rather sharply separated. Nodules are distinguished from concretions by their dominantly silicic composition. Nodules are defined as a small, irregularly rounded knot, mass, or lump of a mineral aggregate, normally having no internal structure, and usually exhibiting a contrasting composition from the enclosing sediment in which it is embedded (Bates and Jackson 1987; in Macsotay et al. 2003). The material presented here is interpreted as concretions, and described as regular and irregularly shaped mineral aggregates of dominantly silicic composition, with visible internal structure, different from that of the rock in which they are hosted.

Marine strata deposited during the Late Cenomanian and Early Turonian commonly display lithological, paleontological, and geochemical characteristics of the oxygen-depleted environment, which mark a geologically short period of around 1 Ma (91.5–90.5 Ma). This event is known as the Cenomanian–Turonian ‘Oceanic Anoxic Event’ (OAE 2 or “Bonarelli event”; Schlanger and Jenkyns

✉ Karmen Fio Firi
karmen.fio@geol.pmf.hr

¹ Croatian Geological Survey, Sachsova 2, 10000 Zagreb, Croatia

² Department of Geology, Faculty of Science, University of Zagreb, Horvatovac 102a, 10000 Zagreb, Croatia

³ Ministry of Environmental and Nature Protection, Radnička cesta 80, 10000 Zagreb, Croatia

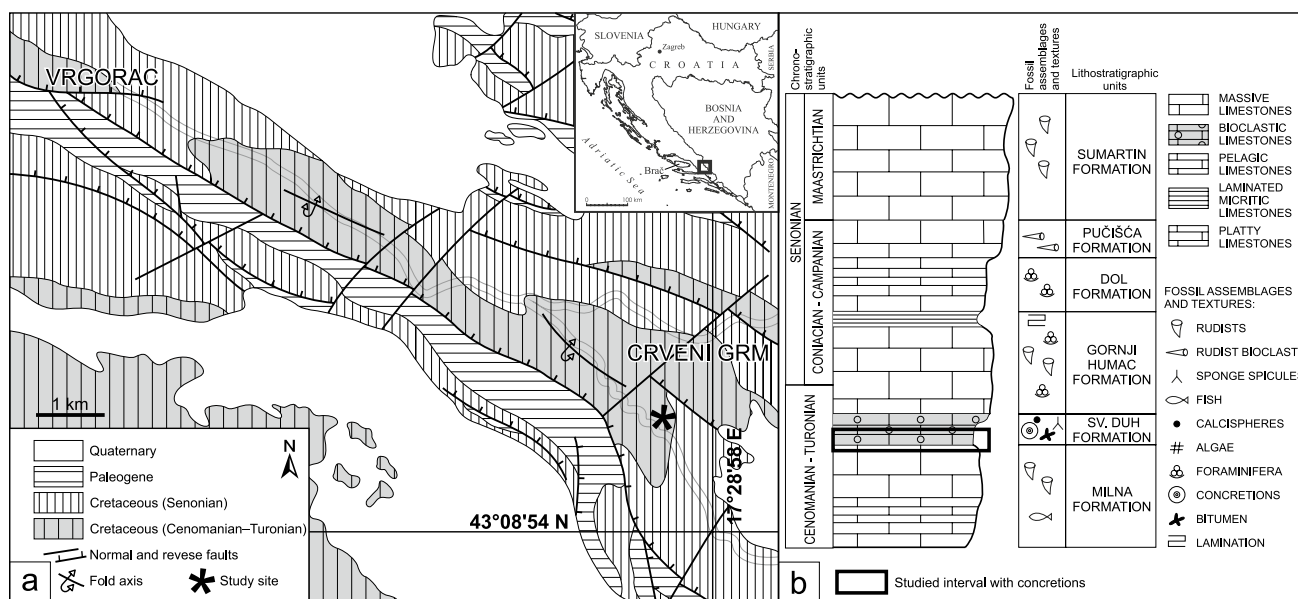


Fig. 1 **a** Simplified geological map of the Pojezerje municipality and surrounding area (modified after Marinčić et al. 1977). The concretions were found in the area of the Šubir hill (marked by asterisk) during tunnel excavations at the highway section Zagreb–Dubrovnik.

b Schematic lithostratigraphic column of the Upper Cretaceous deposits at the Adriatic Carbonate Platform, with marked position of the studied deposits (modified after Marinčić et al. 1977; Jerinić et al. 1994)

1976; Schlanger et al. 1987), or Cenomanian–Turonian Boundary (CTB) event (Jenkyns 1991). Typical deposits are black, pyritic, laminated shales with a high percentage of organic carbon. Coeval pelagic and shelf limestones are lacking dark shales, but are marked by $\delta^{13}\text{C}_{\text{carb}}$ values of 4–5 ‰, which is 2–3 ‰ higher than in the limestones below and above this event (e.g., Schlanger et al. 1987). It is proposed that during the OAE 2 ^{12}C was preferentially extracted from seawater by marine plankton whose organic components were not recycled back into the oceanic reservoir, as a result of enhanced rates of the burial of organic carbon (Schlanger et al. 1987).

Deep-marine limestones containing concretions and radiolarian cherts connected with the Cenomanian–Turonian boundary are known from other parts of the Tethys region, for example the Calabianca section in northwestern Sicily, the Bottaccione section in central Italy (Scopelitti et al. 2004, 2006, 2008), and the Valdagno section in northern Italy (Fig. 2; Coccioni and Luciani 2005). The Rehkogelgraben section in the Austrian Eastern Alps contains pelagic deposits with high planktonic and benthic foraminiferal diversity marking the CTB (Fig. 2; Gebhardt et al. 2010). Pelagic Cenomanian–Turonian limestones are also known from the Trieste-Komen Plateau (Repen Formation) in Slovenia (Fig. 2; Jurkovšek et al. 1996, 2013).

The main aims of this paper are: (1) to determine the petrography of the host rock and spherical concretions, (2) to determine the biostratigraphic position of the host limestones, (3) to identify the source of the silica for the

concretions and explain their origin, (4) to determine differences in growth (shape and composition) of the regular and irregular siliceous concretions, and (5) to define the source of the bituminous material in the host limestones. Stable isotope composition of carbon and oxygen from the zones within the concretions, biomarker composition of bitumen of the surrounding deposits, and mineralogical and paleontological analyses of the host rock and concretions are the methods employed to make these determinations.

Geological setting

During the Mesozoic, the studied area was part of the Adriatic microplate or Adria (Channell et al. 1979; Bosellini 2002). In the Early Jurassic, several carbonate platforms were present in the future peri-Adriatic area, and the Adriatic Carbonate Platform (AdCP; Vlahović et al. 2005), also named Adriatic Dinaridic Carbonate Platform (ADCP; Jelaska 2002) was the largest one (Jenkyns 1991; Gušić and Jelaska 1993; Pamić et al. 1998; Velić et al. 2002).

The studied area of the Pojezerje municipality belongs to the central part of the AdCP, in which Upper Cretaceous succession is generally well developed (Figs. 1, 2). These deposits are described in detail from the island of Brač (marked in Fig. 1a), where six lithostratigraphic units (formations) were proposed (Fig. 1b; Gušić and Jelaska 1990). Pelagic influence can be found within the uppermost Cenomanian–Lower Turonian Sveti Duh Formation and

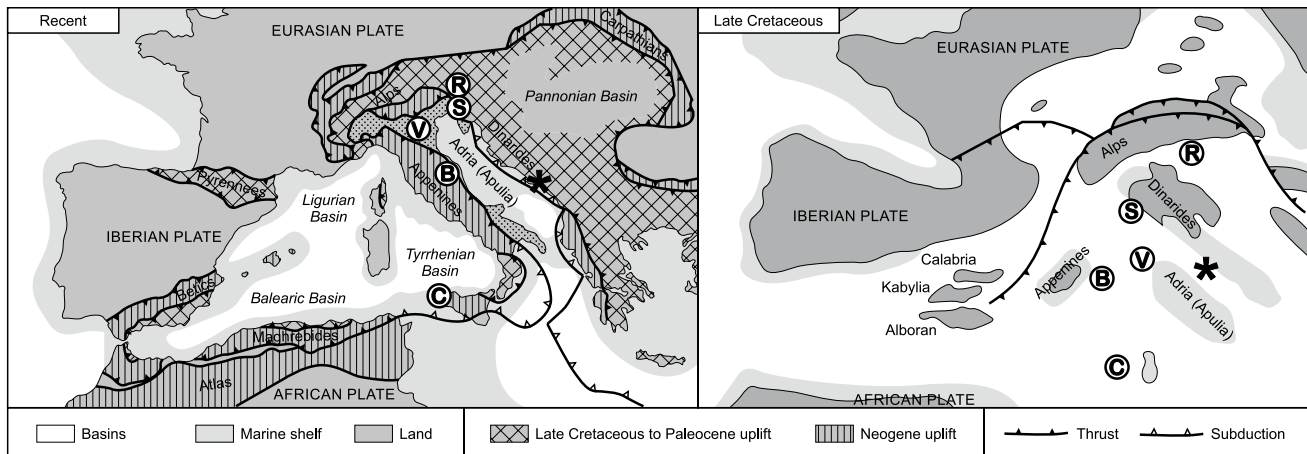


Fig. 2 Simplified map of the Perimediterranean Realm with Recent and Late Cretaceous paleogeographic situation (modified after Cocconi and Luciani 2005; Scopelliti et al. 2006; Benton et al. 2010). Position of the studied deposits is marked by an asterisk. Neighboring sections connected with the Cenomanian–Turonian boundary are

marked with capital letters: *B* Bottaccione section in central Italy, *C* NW Sicilian Calabianca section, *V* Valdagno section in N Italy, *R* The Rehkogelgraben section in the Austrian Eastern Alps, *S* Repen Formation in S Slovenia

Coniacian–Campanian Dol Formation (Gušić and Jelaska 1990; Steuber et al. 2005). The drowning event can be subdivided into three phases: the initiation phase, the maximum drowning phase, and the receding phase. The maximum range of pelagic unit, recognized in the study area, is usually characterized by abundant calcispheres, and ‘primitive’ and opportunistic planktonic foraminifera, with local occurrence of ammonites, pelagic bivalves, and benthic and planktonic echinoderm fragments (Gušić and Jelaska 1993, and references therein). This event has been interpreted to represent an overall sea-level rise that caused pelagic sedimentation on top of the AdCP (Gušić and Jelaska 1990, 1993), and combined influence of local tectonics and global oceanographic perturbations during the Late Cenomanian and Early Turonian time interval (Korbar et al. 2012).

Upper Cretaceous bituminous limestones, which commonly surround the concretions under investigation here, can be found at several neighboring places in the region of Dalmatia (Jerinić et al. 1994, and references therein; Fiket et al. 2008). Bitumen also occurs in surface seepages. Nodules were identified within the bituminous Turonian limestones during the basic geological mapping of Yugoslavia (Marinčić et al. 1977). The new cycle of mapping for the Basic geological map of Croatia 1:300.000 recorded bituminous nodular limestones as the Upper Cenomanian–Lower Turonian deposits (Velić and Vlahović 2009), but the origin of the concretions was not explained until now.

An expression of the Oceanic Anoxic Event OAE 2 at the AdCP, recognizable through stable isotope values of oxygen and carbon ($\delta^{18}\text{O}$ from -2 to -4 , and $\delta^{13}\text{C}$ from $+2$ to $+5$ ‰), was recorded at the island of Brač by Korbar et al. (2012).

Materials and methods

The concretions were first discovered during the excavations of the Šubir hill tunnel at the section of A1 highway Zagreb–Dubrovnik in the Pojezerje municipality area (UTM coordinates $x = 6,457,614$, $y = 4,779,788$; southern Croatia, Fig. 1a), when a large amount of stone “balls” rolled out from the parent rock at several localities. The following fieldwork included identifying the concretions in their autochthonous position within the host limestones, sampling of regularly (Fig. 3a) and irregularly shaped concretions (Fig. 3b), chert bands (Fig. 3c), as well as sampling of the surrounding limestone and bituminous material (Fig. 3b).

The size of the regular concretions varies from only 2 cm up to more than 25 cm in diameter. Zonation of alternating zones, with different carbonate and silica content, and color of the zones, varies from one concretion to the other. With approval of the Ministry of Environmental and Nature protection, two samples were cut in half (marked as K-1 with $d \sim 8$ cm and K-2 with $d \sim 12$ cm; Fig. 4a), to see their inner structure and sample different zones within the concretions.

Five thin-sections made from the concretions were micropaleontologically analyzed in order to find possible siliceous fossils or fossil fragments and to determine the origin of the siliceous material. Morphologic observations of the samples were carried out at the Croatian Geological Survey in Zagreb, with a JEOL JSM-35F scanning electron microscope (SEM) operating in secondary electron mode at an accelerating voltage of 20 kV. The grains were mounted on the SEM stubs and sputtered with gold. The same SEM



Fig. 3 **a** A spherical concretion in autochthonous position (length of the pen is 15 cm). **b** An irregularly shaped concretion within bituminous limestones. **c** Chert bands (length of the pen is 15 cm)

microscope equipped with an Oxford energy dispersive spectrometer (EDS), coupled with an INCA system, was used for elemental distribution analysis in the samples. The EDS qualitative analysis was performed on carbon-coated samples at an accelerating voltage of 20 kV.

To determine the origin of siliceous material, parts of two concretions were dissolved in acetate acid in order to dissolve carbonate material, and in HF to dissolve siliceous material, at the Palaeontological Institute Ivan Rakovac, ZRC SAZU in Ljubljana, Slovenia.

At the Faculty of Science, University of Zagreb, 20 samples of the surrounding rock were prepared as thin-sections for micropaleontological analyses. To determine mineral types (calcite, ferrous calcite, dolomite, ferrous dolomite), samples of the host rock were colored with Alizarin red S and K-ferrocyanide. Calcareous nannoplankton was determined in the samples of the surrounding rocks where other planktonic organisms were observed in light microscopy. Analyses were performed using standard preparation methods, light microscope under polarized and cross-polarized light (Bown and Young 1998), and determined on the basis of Perch-Nielsen (1985).

Material sampled from zones within two cut concretions was used for stable isotope analyses. To analyze stable isotope ratios of carbon and oxygen, the extraction of CO₂ was done in a Carbonate Kiel Device III (Thermo Finnigan) at the University of Barcelona, Spain, which uses an automated version of the McCrea (1950) method. Carbonate was attacked with 100 % phosphoric acid at 70 °C, with a reaction time of 3 min for calcite. The Carbonate Kiel Device is coupled to an isotope ratio mass spectrometer MAT-252 (Thermo Finnigan), in which the produced CO₂ was analyzed. In order to control the quality of the results, the NBS-19 international standard was used, with $\delta^{13}\text{C}$ (PDB) = +1.95 ‰ and $\delta^{18}\text{O}$ (PDB) = -2.20 ‰ values, certified by the IAEA. The standard deviation for the

standards (σ parameter, used as a method reproducibility indicator) was 0.04 for $\delta^{13}\text{C}$ and 0.12 for $\delta^{18}\text{O}$.

Bitumen extraction was done at the INA d.d. in Zagreb. Extractable organic matter of the powdered rock sample was determined by the 36-h Soxhlet extraction with chloroform. The extract was then separated by the column liquid chromatography into four fractions: saturated hydrocarbons (alkanes), aromatic hydrocarbons, NSO-compounds, and asphaltthenes. Gas chromatography analyses of the alkane fraction were performed on a Perkin Elmer Sigma 300 and Varian 3900 GC. For monitoring *n*-alkanes *m/z* ion 71 was used, acyclic izoprenoids *m/z* 113, for triterpanes *m/z* 191 and for steranes *m/z* 217 and 218.

Results

Petrography of the concretions and the surrounding rocks

Studied concretions are mostly regularly shaped, with aspect ratio less than 1.5:1. These spheroid concretions show extensive zonation, with alternating zones of differing carbonate and silicate content (Fig. 4a). Irregularly shaped concretions (Fig. 3b) and chert bands (Fig. 3c) are also present within the studied deposits and are almost entirely composed of the siliceous component. Due to the diagenesis, central parts of the concretions exhibit numerous rhombohedral dolomite crystals within the quartz matrix (Fig. 4b, d). The dolomite crystals are post-diagenetically completely or partially dissolved and now mostly preserved only as remains in rhombohedral moulds resembling dissolved crystals. The EDS analysis of the mineral remains in the moulds shows dolomite composition (Fig. 4d). The zones towards the edge of the concretions contain numerous well-visible siliceous sponge spicules, which are

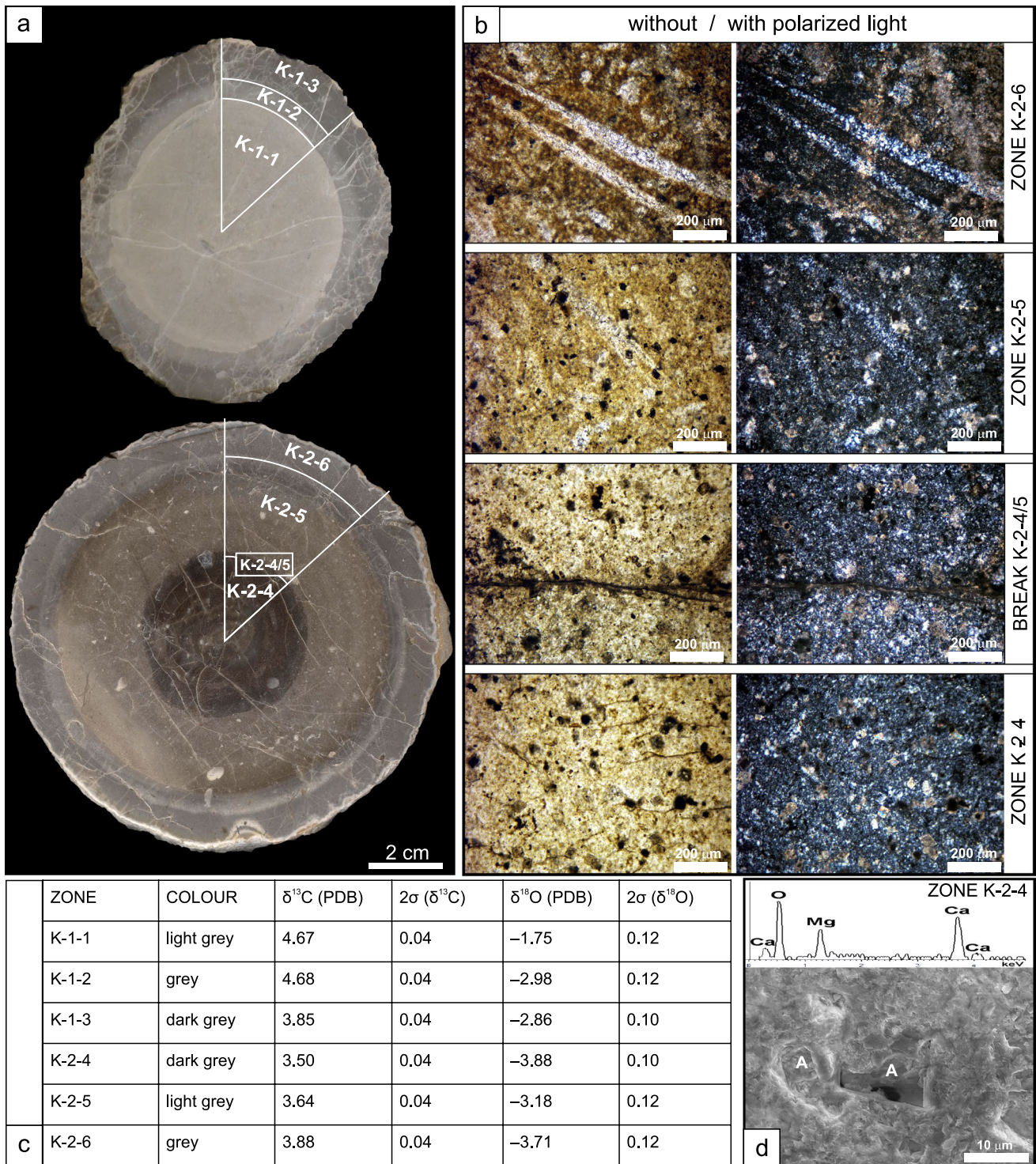


Fig. 4 **a** Spheroid concretions with visible zonation (alternating zones with different carbonate and silicate content). **b** Photomicrographs showing visible gradual devastation of the sponge spicules from the central part (zone K-2-4), towards the edge of the bigger concretion (zone K-2-6). Note that there is a visible break between

two zones, marked here between the fourth and fifth zone, as K-2-4/5. **c** Table with the coloring and stable isotope composition ($\delta^{13}\text{C}_{\text{carb}}$ and $\delta^{18}\text{O}_{\text{carb}}$) of the zones within concretions. **d** A SEM image of the zone K-2-4 showing dolomite rhombohedra in the opal matrix and corresponding EDS analysis (the A marks points of analysis)

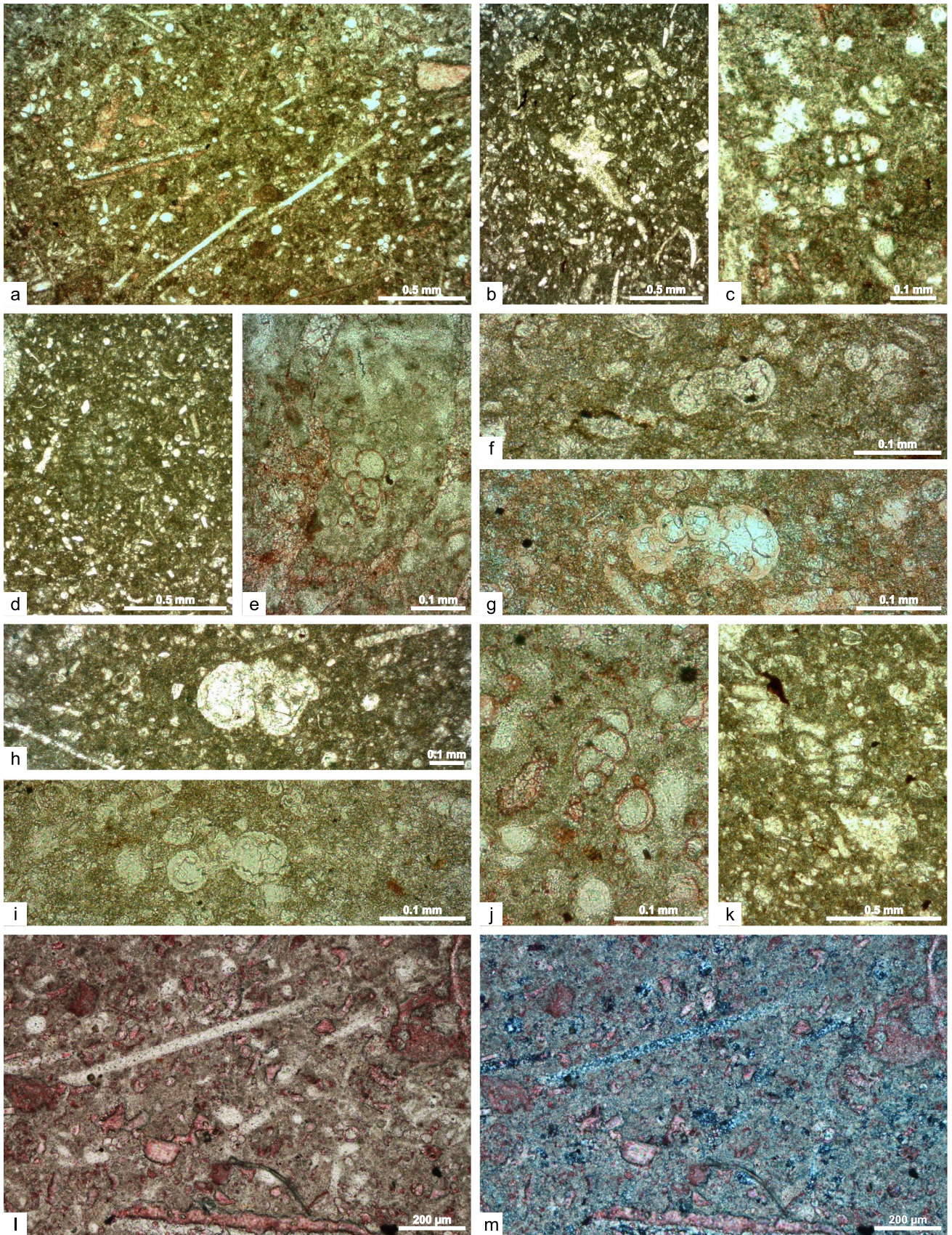


Fig. 5 Photomicrographs of the limestones surrounding the concretions indicating microfacies types and microfossil assemblages. **a** Bioclastic packstone with sponge spicules and echinoderm debris. **b** Bioclastic packstone with sponge spicules and crinoid remains. **c** Bioclastic wackestone to packstone with calcispheres and fragments of benthic foraminifera *Moncharmontia* cf. *compressa* De Castro. **d** Bioclastic wackestone to packstone with calcispheres and fragments of *Cuneolina* sp. **e–i** Planktonic foraminifera: **e** *Heterohelix reussi* (Cushman), **f, g** *Wittheinella aprica* (Loeblich and Tappan), **h** *Wittheinella* sp. **i** *Globigerinelloides bollii* (Pessagno). **j** *Bulimina* sp. **k** *Gaudryna* sp. **l–m** Siliceous monaxon sponge spicules (longitudinal and transverse sections) without (**l**) and with crossed nicols (**m**)

recrystallized into quartz, but with perfectly preserved morphology (Fig. 4b).

The prevailing composition of the surrounding rocks and most of the fossil content is calcite, which was noted due to the coloring of thin-sections. The sedimentary rocks surrounding the concretions are wackestones-packstones with abundant calcispheres, planktonic foraminifera, sponge spicules, and echinoderm fragments. The outer surface of the concretions and surrounding host sedimentary rocks are often impregnated with bituminous material (Fig. 3b).

Biostratigraphy

The most abundant fossils in mud-supported limestones (bioclastic wackestones and packstones) are calcispheres, small-sized planktonic foraminifera, sponge spicules (Fig. 5a), echinoderm debris, and rare crinoid fragments (Fig. 5b). In high concentrations these skeletal fragments form bioclastic calcarenites (bioclastic packstones). Sometimes these packstones contain bioclasts of shallow-water platform carbonates, which contain the Late Cretaceous benthic foraminifera *Moncharmontia* cf. *compressa* De Castro (Fig. 5c) and *Cuneolina* sp. (Fig. 5d). The presence of planktonic foraminifera assemblages, consisting of *Heterohelix reussi* (Cushman) (Fig. 5e), *Wittheinella aprica* (Loeblich and Tappan) (Fig. 5f, g), *Wittheinella* sp. (Fig. 5h), *Globigerinelloides bollii* (Pessagno) (Fig. 5i), and rare small benthic foraminifera, *Bulimina* sp. (Fig. 5j) and *Gaudryna* sp. (Fig. 5k), indicate latest Cenomanian–Early Turonian age. Such microfacies and microfossil assemblage characterize the Sveti Duh Formation (Fig. 1b), which can be easily recognized in the Dalmatian part of the AdCP.

Siliceous fragments are visible in thin-sections prepared from both the surrounding rocks and within the concretions, and the most abundant remains belong to sponge spicules (Figs. 4b, 5l, m). The only found calcareous nanoplankton belongs to the species *Watznaueria barnesiae* (Black in Black and Barnes, 1959) Perch-Nielsen, 1968. This species is quite resistant, even to the diagenetic processes, with stratigraphic range from Middle Jurassic to the end of Cretaceous (Perch-Nielsen 1985).

Source of silica

In the limestone thin-sections, numerous leached siliceous monaxon sponge spicules were recognized in different sections, usually transverse and rare longitudinal (Figs. 4b, 5l, m). Beside siliceous sponges, possible sources of silica could be other opal-A secreting marine organisms like radiolarians, diatoms, or silicoflagellates. Meteoric water charged with silica may also provide the amount of material needed for the growth of concretions, but no evidence for this presumption was found.

Stable isotopes (carbon and oxygen) from the concretions

The zones within the concretion were sampled from nucleus outwards and marked by numbers K-1-1 to K-1-3 for the smaller sampled concretion, and K-2-4 to K-2-6 for the bigger one (Fig. 4a, b).

There is a difference in carbon and oxygen isotope values between different zones within the concretion (inner and outer parts). The stable isotope values show no trend from the nucleus outwards. The lightest grey zones are represented by higher positive values of the $\delta^{13}\text{C}_{\text{carb}}$, while the darkest zones show lower $\delta^{13}\text{C}_{\text{carb}}$ ratios.

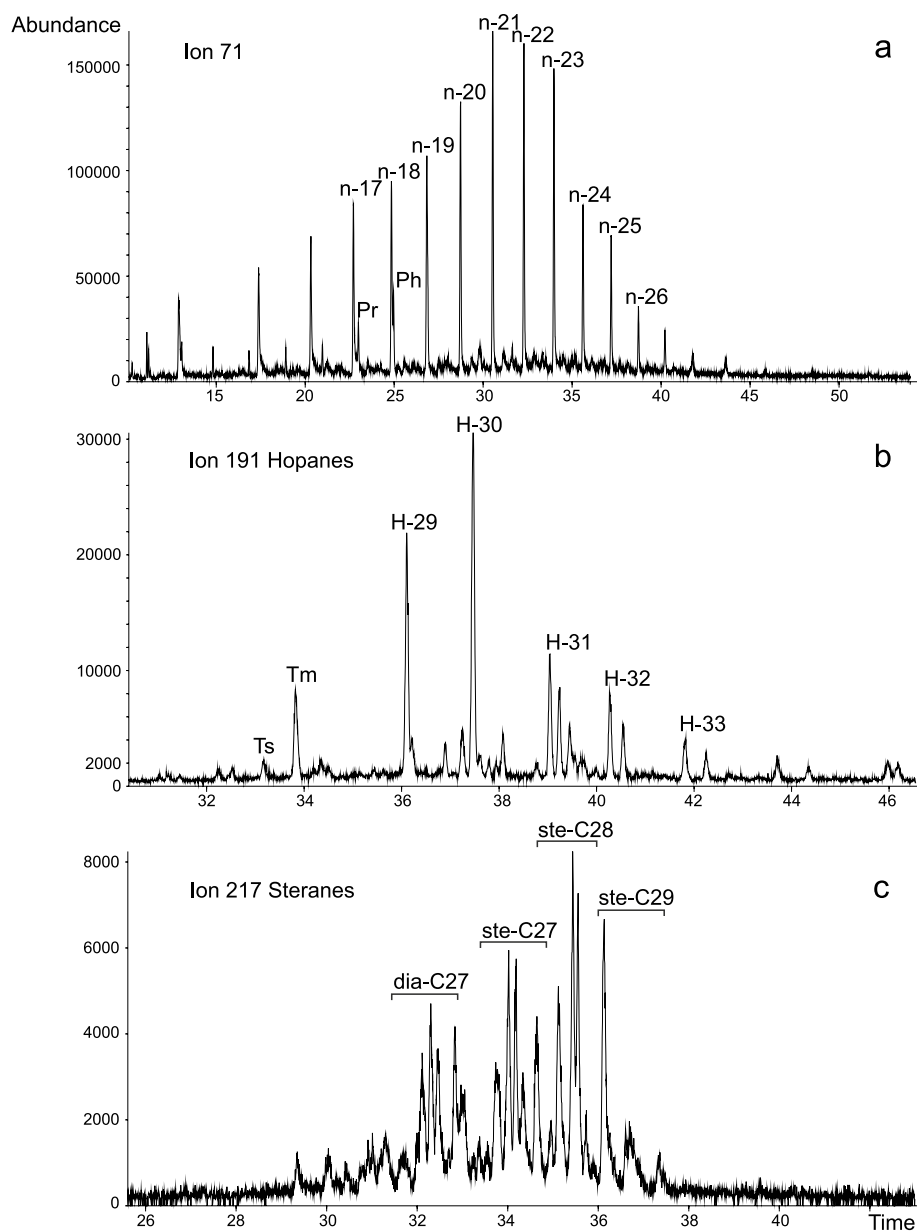
The smaller concretion (K-1; Fig. 4a, c), with an inner zone showing light grey color, and grey and dark grey zone towards the outer edge, shows an almost constant value of the $\delta^{13}\text{C}_{\text{carb}}$ for the first and second zone (+4.67 ‰ and 4.68 ‰), while the outermost zone exhibits lower values ($\delta^{13}\text{C}_{\text{carb}} = +3.85$ ‰). The bigger concretion (K-2; Fig. 4a, c) also consists of three main zones, with an innermost zone of dark grey, a middle zone light grey, and grey outermost zone. The innermost zone shows $\delta^{13}\text{C}_{\text{carb}}$ of 3.50 ‰, while the middle zone displays values almost exactly the same as the inner and middle part of the smaller concretion (4.64 ‰). In contrast, the outermost zone preserves a $\delta^{13}\text{C}_{\text{carb}}$ of 3.88 ‰ (comparable to 3rd zone of the smaller concretion).

The $\delta^{18}\text{O}$ ratios vary from -1.75 to -2.98 ‰ for the smaller and from -3.18 to -3.88 ‰ for the bigger concretion (Fig. 4c), exhibiting recognizable values for the globally detected OAE 2 at the AdCP ($\delta^{18}\text{O}$ from -2 to -4 ‰; Korbar et al. 2012).

Biomarker analyses

One bitumen sample from the parent rock was extracted for the biomarker analyses. The main extractable compounds belong to four main groups, namely *n*-alkanes, acyclic isoprenoids (e.g., pristane, phytane), steroids, and hopanoids, in variable relative amounts.

Fig. 6 Ion chromatograms for the saturated fraction of the bitumen sample: **a** m/z 71 with normal alkanes, and pristane and phytane. **b** Expanded m/z 191 showing the distribution of hopanes. **c** Expanded m/z 217 showing the distribution of steranes



The C-chain lengths of normal alkanes in our sample range from C_{17} to C_{26} , maximizing at C_{21} (Fig. 6a). Normal alkanes C_{15} , C_{17} , C_{19} and C_{22} are usually algal biomarkers, pointing to a marine environment, while mid-chained n -alkanes (C_{16} – C_{20}) are usually cyanobacterial biomarkers in the sedimentary organic matter (Grimalt and Albaigés 1987; Maliński et al. 2009, and references therein).

From the acyclic isoprenoids, only pristane (C_{19} , Pr) and phytane (C_{20} , Ph) are present (Fig. 6a). The Pr/ n - C_{17} value of 0.338 and Ph/ n - C_{18} value of 0.392 point to marine type of organic matter from carbonate rocks. The value of 0.86 for the Pr/Ph ratio points to the marine type of organic matter, deposited under anoxic conditions (Didyk et al. 1978).

In the saturated hydrocarbon fractions, hopanes are derived from bacteria, and are detected in the m/z 191 ion chromatogram. Steranes are derived from algae and higher plants, and detectable in the m/z 217 and 218 ion chromatogram (e.g., Peters et al. 2005). Hopanes are most abundant in range from C_{29} to C_{33} (Fig. 6b). Hopanes C_{27} to C_{40} are biomarkers for bacteria, or even pelagic cyanobacteria, marking the anoxic marine environment (Peters et al. 2005). Organic matter-rich sediments of OAE 2, under conditions of prolonged ocean stratification, increased rates of organic-carbon accumulation and high nutrient-N, were dominant by N_2 -fixing cyanobacteria (Karakitsios et al. 2007, and references therein). Steranes are ranging from

dia-C₂₇ to ste-C₂₉, with most abundant ste-C₂₈ (Fig. 6c) marking marine type of organic matter.

Discussion

In our studied area, the deposits of the uppermost Cenomanian–Lower Turonian Sveti Duh Formation, surrounding the concretions, indicate pelagic incursion over the platform, specifically the drowning of the AdCP. The limestones in which the concretions were found are not texturally or compositionally different from deposits in which concretions were not detected. The concretions themselves, as mineral bodies, differ in composition from the rock in which they were formed, commonly limestones and dolomites.

Stable isotopes from the concretions

Pelagic carbonates of the Cenomanian–Turonian boundary are generally represented by a positive excursion in $\delta^{13}\text{C}_{\text{carb}}$, which reflects changes in the $\delta^{13}\text{C}$ of the oceanic total dissolved carbon, due to the increase in the burial ratio of organic carbon to CaCO_3 (Arthur et al. 1987). The values between 3.50 and 4.68 ‰ for $\delta^{13}\text{C}_{\text{carb}}$ correspond well to the globally known carbon isotope values for the Cenomanian–Turonian event (4–5 ‰, Schlanger et al. 1987). Zones within the concretions are characterized by different $\delta^{13}\text{C}$ values, suggesting that they did not all grow at the same time but over longer period during which water composition varied (cf. McBride et al. 1999). The measured carbon isotope ratios suggest that zones with similar isotope values have grown during similar environmental conditions or temperatures, or have been exposed to similar diagenetic conditions.

Oxygen isotope ratios in the concretions range from –1.75 to –3.88 ‰, and can be considered as a reflection of the Oceanic Anoxic Event at the AdCP, as previously recorded by Korbar et al. (2012). Differences in the oxygen isotope ratios point to: (1) possible changes in temperature during the formation of the different zones, (2) if the temperature was constant, that the nucleus of the smaller concretion formed from the water with heavier $\delta^{18}\text{O}$ than the margins, while the nucleus of the bigger concretion formed from the water with lighter $\delta^{18}\text{O}$ than the margins (cf. McBride et al. 1999), or (3) possible diagenetic changes. Much of the Mesozoic–early Paleogene time was globally warm and the oceanic bottom waters were quite different than today, due to the absence of polar deep-water masses (Arthur et al. 1987, and references therein). These warm bottom waters could have influenced the formation of spherical concretions. Nevertheless, the change in oxygen isotope ratios of different zones, with range of values

from –1.8 to –3.9 ‰, can also be explained through a possible diagenetic influence.

Growth of the concretions

We propose that the growth of the concretions took place from the nucleus outwards, with silica being scavenged from the surrounding sediment to feed the growing concretion. The cement of the spherical concretions was supplied by diffusion during concretion growth (McBride et al. 1999, and references therein). In case of elongated concretions, the cement was supplied by advection, showing the direction of the fluid flow. Alternating zonation of opal- and carbonate-rich zones derive from fast “consummation” of silica material at the growth site.

Calcium source is not questionable here; Ca is most probably sourced by dissolution from the concretion host sediment, which is mainly composed of calcite detritus.

The silicate component of the concretions originates from biogenic opal, mainly sponge spicules (Figs. 4b, 5l, m) and probable radiolarians. Biogenic silica (opal-A) is amorphous, hydrated, and is the most unstable form of silica. It is experimentally shown that solubility of opal-A silica strongly depends on environment pH and silica saturation (Lewin 1961; Badut and Risacher 1983). Biogenic opal is altered only at pH 8.5 and higher.

If we overlap geochemical stability fields of calcite and biogenic opal, it is evident that in an environment with elevated pH, biogenic opal will dissolve, while calcite will precipitate.

Carbonate precipitation on the opal surface is strongly enhanced due to the cation adsorption on dissociated silanol groups –SiOH (Dixit and Van Cappelen 2002). Silanol groups on biogenic silica surface are known as excellent ligands for aluminium, calcium, iron, and other cations existing in sediment pore waters (Schindler and Stumm 1987). It is important to emphasize that there are two different growth mechanisms for opal and carbonate additionally enhancing zone formation during the concretion formation and preferring different opal or carbonate content in one zone layer. Carbonate mineral formation in the sediment as cement is a result of the crystallization process from an oversaturated solution, while silica gels form by polymer flocculation (Stumm 1993). In the case of the concretions described here, crystallization of silica appears later during the diagenesis, resulting in quartz mineralization. Carbonate precipitation could be slowed down or stopped, due to inhibition by adsorbed organic matter or sulphate on possible carbonate crystal nucleation sites (Berner et al. 1978). From numerous previous research (e.g., Berner et al. 1978; Raiswell 1988), there is evidence that such surface-reaction mechanisms can have significant control over carbonate concretion growth.

It is important to notice that surface adsorption of organic matter or sulphate on carbonate or silicate nucleation sites could, in our case, only periodically slow down concretion growth. The explanation for the periodic growth could be in microbial sulphate reduction by organic matter (Raiswell 1976; Raiswell and Fisher 2000). In this manner, the crystal nucleation sites could be liberated for further concretion growth, until new contamination with sulphate and organic matter occurs. Additionally, sulphate reduction generates alkalinity (Coleman 1993; Coleman and Raiswell 1995), which could lead to carbonate super-saturation and initiate concretion growth.

If we propose that the source of silica is mostly biogenic opal-A (siliceous sponges, and possibly radiolarians, diatoms, and silicoflagellates), what would the initial concentration of those organisms be? Calculations by McBride et al. (1999, and references therein), indicated that deep-sea deposits can contain up to 30 % of opaline biogenic grains, which would be enough to form the concretions. Even in modern carbonate deposits, opal-A secreting organisms are present in large enough amounts to provide silica for chert nodules (McBride et al. 1999).

Partial consolidation of sediments and preferential orientation of platy-shaped sediment particles would cause greater horizontal than vertical sediment permeability and a slight preferential transport horizontally, giving the characteristic oblate sphere concretion shape. All apparently irregular concretion shapes are in fact typical for gel structures, resembling geometrical shapes of minimal surface tension (energy). The silica that formed the chert bands had to migrate to the sites of precipitation by diffusion, while CaCO_3 released by the replacement process had to diffuse outwards or precipitate as cement in the limestones. This process could be one of the possible explanations for the rhythmic banding of the concretions. During the growth of the concretion, uneven diffusion process results in irregular-shaped concretions. In the case of spherical concretions, their growth is favored by sediments of homogenous texture and composition (McBride et al. 1999).

Biogenic silica (opal-A) is amorphous, hydrated, and the most unstable form of silica and its solubility greatly increases with temperature, pressure, solution under-saturation, and pH elevation (Lewin 1961). Typical marine early-diagenetic carbonate environments with elevated pH contain less dissolved silica than could be possible; they are under-saturated with respect to silica, resulting in fast dissolution of biogenic opal remains (Kröger and Sumper 2000). The dissolution-precipitation reaction of biogenic silica can be shown with the formula: $\text{SiO}_2 + 2\text{H}_2\text{O} \leftrightarrow \text{Si(OH)}_4$. Fast dissolution of opal-A, and stagnant pore waters, yields solutions of relatively high silica content. In pore waters saturated with silica, open-framework silica polymers form and flocculate to yield opal-CT. Once

emplaced as a proto-concretion, such globular molecular cluster starts to grow in the direction of the new material supply. A highly spherical concretion shape indicates the same supply rate of the source material from all directions. Such conditions can be established in stagnant sediment pore waters where material supply at the growth site comes only from molecular diffusion. The efficiency of diffusion is determined by the diffusion coefficient, the permeability, and the concentration gradient. Diffusion is one of the most important processes acting during sediment diagenesis and especially concretion growth (Berner 1971). With the formation of the core, the growth starts, and source material concentration gradient is established. A concentration gradient results in an ion flux from the surrounding sediment toward the growth site, which leads to the ion-depleted zone in the near concretion volume.

Diagenetic processes affect the preservation of siliceous material, in this case sponge spicules, within the matrix of the concretions, and this process can be followed from the center outwards. Outer zones contain remnants of preserved spicules, while those in the inner parts are not preserved (Fig. 4b). Due to the dissolution of the spicules, the calcite matrix was replaced by the authigenic (chemogenic) dolomite, which is the most abundant in the innermost zones of the concretions (Fig. 4b, d). This can be explained in regards to the silanol groups. The surface part of the sponge spicules in the alkali environment becomes negatively charged (silanol groups). This kind of ionized surface adsorbs cations from the solution, e.g., magnesium from the sea water. With the change of the opal-A into the more stable forms (opal-CT and quartz), cations are released, and, in this case, magnesium precipitates into dolomite crystals. The innermost zone of the concretion (zone K-2-4, Fig. 4a, b) therefore shows numerous rhombohedral dolomite crystals within the quartz matrix. The second zone shows a silicified matrix with gradual devastation of siliceous spicules, with better-preserved morphology of the spicules going towards the edge of the concretions (zone K-2-5; Fig. 4a, b). In the outermost part of the concretion (zone K-2-6, Fig. 4a, b), numerous siliceous sponge spicules are still visible, and even though they are recrystallized into quartz, their morphology is perfectly preserved.

Bitumen from the host rock

Preservation of bituminous material in carbonates is connected with stagnant pore waters and rapid sea-level rise due to the Oceanic Anoxic Event (OAE) at the Cenomanian–Turonian transition (Gušić and Jelaska 1990, 1993, and references therein). The Upper Cretaceous oil-seep deposits from the Vrgorac area (Fig. 1) are generally represented by carbonates with pores, fissures, and cavities, which are filled with the migrated bitumen (Fiket et al. 2008).

Due to the OAE conditions, the bottom waters were nutrient-rich and oxygen-poor and differing in temperature from the surface waters. Due to the light color of the rocks, and comparison with the Sveti Duh Formation, it is presumed that the depth where the concretions were formed could not be bathyal or abyssal, but that deposition took place in the oxygen-depleted environments of the drowned platform succession.

The presence of biomarkers, including *n*-alkanes C₁₇–C₂₆, pristane (Pr), phytane (Ph), C₂₉–C₄₀ hopanes, and dia-C₂₇ to C₂₉ steranes (Fig. 6) point out that the dominant sources of organic matter throughout the column were marine biota (mainly algae, bacteria, and cyanobacteria). Late Cenomanian–Early Turonian transgression led to the supply of additional nutrients to the platform, which enhanced the paleoproductivity and, owing to the decay of organic matter, led to the increased consumption of O₂ (cf. Lebedel et al. 2013).

Conclusions

1. We present a new find of mostly spherical concretions from southern Croatia, which exhibit variable carbonate and, dominantly, siliceous composition, with the visible internal structure, differing from the parent rocks. Silica was provided by diffusion, while carbonate material probably precipitated as cement in the limestones.
2. The sedimentary rocks surrounding the concretions are wackestones and packstones with abundant calcispheres, planktonic foraminifera, rare benthic foraminifera, sponge spicules and echinoderm fragments, whose presence is typical for the pelagic Cenomanian–Turonian Sveti Duh Formation of the Adriatic Carbonate Platform.
3. We argue that the main sources of silica were siliceous sponges, with possible influence of other opal-A secreting marine organisms like radiolarians, diatoms, or silicoflagellates. Diagenetic processes have influenced zonal growth within the concretions in the way that siliceous spicules, as source of silica, are completely dissolved within the concretion nucleus.
4. The $\delta^{13}\text{C}_{\text{carb}}$ values of the zones within the concretions range from 3.50 to 4.68 ‰ and correspond well to the globally known carbon isotope values for the Cenomanian–Turonian OAE 2 event.
5. The presence of biomarkers, including *n*-alkanes C₁₇ to C₂₆, pristane, phytane, C₂₉ to C₄₀ hopanes and dia-C₂₇ to C₂₉ steranes point to the dominant sources of organic matter for the bitumen deposition as algae, bacteria, and cyanobacteria.
6. The siliceous-carbonate concretions described here and the mechanisms of their growth do not depend on certain time and space, and therefore represent excellent and rare example where natural laws governing shaping and appearance of matter can be clearly seen and successfully used to explain the occurrence of geological phenomena. We would like to encourage similar findings in the world, to explain this phenomenon and its connection with stress events in the geological record.

Acknowledgments We would like to thank the first finder of this phenomenon M. Martinović, writer and journalist J. Divić from Vrgorac, Pojezerje municipality area and Public Institution for Management of Protected Natural Values in the Dubrovnik-Neretva County for bringing us closer to this phenomenon. Concretions are preserved ex situ by the Croatian Ministry of Environmental and Nature protection (former Ministry of Culture) by the Nature Protection Directorate since 2011. For help in analytical process, we would like to thank D. Kukoč (for Radiolaria) and Š. Aščić (calcareous nannoplankton) from University of Zagreb, and T. Troškot-Čorbić from INA d.d. (for biomarkers). To the University of Barcelona, we are thankful for providing the laboratory for stable isotope analyses. We are grateful to R. Koščal (University of Zagreb) for preparation of graphics. For language improvements, we would like to thank Dr. Robyn Pickering (Faculty of Science, University of Cape Town, South Africa). This study was supported by the Croatian Ministry of Science, Education and Sports, project number 119-1951293-1162. We would like to thank Axel Munnecke, Editor-in-Chief, and two anonymous reviewers, for their constructive comments on the manuscript.

References

- Arthur MA, Schlanger SO, Jenkyns HC (1987) The Cenomanian/Turonian Oceanic Anoxic Event, II: paleoceanographic controls on organic matter production and preservation. In: Brooks J, Fleet AJ (eds) Marine petroleum source rocks. Geological Society Special Publication, no 26. Geological Society, London, pp 401–420
- Badut D, Risacher F (1983) Authigenic smectite on diatom frustules in Bolivian saline lakes. *Geochim Cosmochim Acta* 47:363–375
- Bates RL, Jackson JA (1987) Glossary of geology, 3rd edn. American Geological Institute, Alexandria, p 788
- Benton MJ, Csiki Z, Grigorescu D, Redelstorff R, Sander PM, Stein K, Weishampel DB (2010) Dinosaurs and the island rule: the dwarfed dinosaurs from Hațeg Island. *Palaeogeogr Palaeoclimatol Paleoecol* 293(3–4):438–454. doi:10.1016/j.palaeo.2010.01.026
- Berner RA (1971) Principles of chemical sedimentology. McGraw-Hill Inc, New York, p 240
- Berner RA, Westrich JT, Graber R, Smith J, Martens C (1978) Inhibition of aragonite precipitation for supersaturated sea-water: a laboratory and field study. *Am J Sci* 278:816–837
- Bosellini A (2002) Dinosaurs “rewrite” the geodynamics of the eastern Mediterranean and paleogeography of the Apulia platform. *Earth-Science Reviews* 59:211–234
- Bown PR, Young JR (1998) Techniques. In: Bown PR (ed) Calcareous nannofossil biostratigraphy. Chapman & Hall, Cambridge, pp 16–28
- Channell JET, D’Argenio B, Horvath F (1979) Adria, the African promontory, in Mesozoic Mediterranean palaeogeography. *Earth Sci Rev* 15:213–292

- Coccioni R, Luciani V (2005) Planktonic foraminifers across the Bonarelli Event (OAE2, latest Cenomanian): the Italian record. *Palaeogeogr Palaeoclimatol Paleoecol* 224:167–185. doi:[10.1016/j.palaeo.2005.03.039](https://doi.org/10.1016/j.palaeo.2005.03.039)
- Coleman ML (1993) Microbial processes: controls on the shape and composition of carbonate concretions. *Mar Geol* 113:127–140
- Coleman ML, Raiswell R (1995) Source of carbonate and origin of zonation in pyritiferous carbonate concretions: evaluation of a dynamic model. *Am J Sci* 295:282–308
- Didyk BM, Simoneit BRT, Brassell SC, Eglinton G (1978) Organic geochemical indicators of palaeoenvironmental conditions of sedimentation. *Nature* 272:216–222
- Dixit S, Van Cappelen P (2002) Surface chemistry and reactivity of biogenic silica. *Geochim Cosmochim Acta* 66:2559–2568
- Fiket Ž, Alajbeg A, Strmić Palinkaš S, Tari-Kovačić V, Palinkaš L, Spangenberg J (2008) Organic geochemistry of Jurassic-Cretaceous source rocks and oil seeps from the profile across the Adriatic-Dinaric carbonate platform. *Geol Carpath* 59(3):225–236
- Gebhardt H, Friedrich O, Schenk B, Fox L, Hart M, Wägrich M (2010) Paleooceanographic changes at the northern tethyan margin during the Cenomanian–Turonian Oceanic Anoxic Event (OAE-2). *Mar Micropaleontol* 77:25–45. doi:[10.1016/j.marmicro.2010.07.002](https://doi.org/10.1016/j.marmicro.2010.07.002)
- Grimalt J, Albaigés J (1987) Sources and occurrence of C_{12} – C_{22} *n*-alkane distribution with even carbon-number preference in sedimentary environments. *Geochim Cosmochim Acta* 51:1379–1384
- Gušić I, Jelaska V (1990) Upper Cretaceous stratigraphy of the island of Brač. *Yugoslavian Academy of Science and Arts* 69, Zagreb, p 160
- Gušić J, Jelaska V (1993) Upper Cenomanian–Lower Turonian sea-level rise and its consequences on the Adriatic-Dinaric carbonate platform. *Geol Rundsch* 82:676–686
- Jelaska V (2002) Carbonate Platforms of the External Dinarides. In: Vlahović I, Tišljarić J (eds) *Evolution of Depositional Environments from the Palaeozoic to the Quaternary in the Karst Dinarides and Pannonian Basin*. 22nd International Association of Sedimentologists, Meeting of Sedimentology, Opatija, Field Trip Guidebook, pp 67–71
- Jenkyns HC (1991) Impact of Cretaceous sea-level rise and anoxic events on the Mesozoic carbonate platform of Yugoslavia. *Am Assoc Pet Geol Bull* 75:1007–1017
- Jerinić G, Jelaska V, Alajbeg A (1994) Upper Cretaceous organic-rich laminated limestones of the Adriatic Carbonate Platform, Island of Hvar, Croatia. *AAPG Bulletin* 78:1313–1321
- Jurkovšek B, Toman M, Ogorelec B, Šribar L, Drobne K, Poljak M, Šribar Lj (1996) Geological map of the southern part of the Trieste-Komen plateau—Cretaceous and Paleogene carbonate rocks. *Inštitut za geologijo, geotehniko in geofiziko, Ljubljana*, p 143
- Jurkovšek B, Cvetko Tešović B, Kolar-Jurkovšek T (2013) *Geology of Kras (Geologija Krasa)*. Geological Survey of Slovenia, Ljubljana, p 205
- Karakitsios V, Tsikos H, van Breugel Y, Koletti L, Sinninghe Damsté JS, Jenkyns HC (2007) First evidence for the Cenomanian–Turonian Oceanic Anoxic Event (OAE2, ‘Bonarelli’ event) from the Ionian Zone, western continental Greece. *Int J Earth Sci (Geol Rundsch)* 96:343–352. doi:[10.1007/s00531-006-0096-4](https://doi.org/10.1007/s00531-006-0096-4)
- Korbar T, Glumac B, Cvetko Tešović B, Cadieux SB (2012) Response of a carbonate platform to the Cenomanian–Turonian drowning and OAE2: a case study from the Adriatic platform (Dalmatia, Croatia). *J Sediment Res* 82:163–176. doi:[10.2110/jvsr.2012/17](https://doi.org/10.2110/jvsr.2012/17)
- Kröger N, Sumper M (2000) The biochemistry of silica formation in diatoms. In: Bäuerlein E (ed) *Biomining—From biology to biotechnology and medical application*. Wiley, Weinheim, pp 151–170
- Lebedel V, Lezin C, Andreu B, Wallez M-J, El Ettachfani M, Riquier L (2013) Geochemical and palaeoecological record of the Cenomanian–Turonian Anoxic Event in the carbonate platform of the Preafrican Trough, Morocco. *Palaeogeogr Palaeoclimatol Paleoeol* 369:79–98. doi:[10.1016/j.palaeo.2012.10.005](https://doi.org/10.1016/j.palaeo.2012.10.005)
- Lewin JC (1961) The dissolution of silica from diatom walls. *Geochim Cosmochim Acta* 21:182–198
- Macsotay O, Erlich RN, Peraza T (2003) Sedimentary structures of the La Luna, Navay and Querecural Formations, Upper Cretaceous of Venezuela. *Palaios* 13:334–348
- Maliński E, Gąsiewicz A, Witkowski A, Szafranek J, Pihlaja K, Oksman P, Wiinamäki K (2009) Biomarker features of sabkha-associated microbialites from the Zechstein Platy Dolomite (Upper Permian) of northern Poland. *Palaeogeogr Palaeoclimatol Paleoeol* 273:92–101. doi:[10.1016/j.palaeo.2008.12.005](https://doi.org/10.1016/j.palaeo.2008.12.005)
- Marinčić S, Magaš N, Benček Đ (1977) *Basic Geological Map of SFRY 1:100,000*. Ploče Sheet. State Geological Institute, Beograd
- McBride EF, Abdel-Wahab A, El-Younsy ARM (1999) Origin of spheroidal chert nodules, Drunka Formation (Lower Eocene). *Egypt. Sedimentology* 46:733–755
- McCrea JM (1950) On the isotope chemistry of carbonates and paleotemperature scale. *J Chem Phys* 18:849–857
- Pamić J, Gušić I, Jelaska V (1998) Geodynamic evolution of the Central Dinarides. *Tectonophysics* 297:251–268
- Perch-Nielsen K (1985) Mesozoic calcareous nannofossils. In: Bolli HM, Saunders JB, Perch-Nielsen K (eds) *Plankton stratigraphy*. Cambridge University Press, Cambridge, pp 329–426
- Peters KE, Walters CC, Moldowan JM (2005) *The biomarker guide*. Cambridge University Press, Cambridge, p 471
- Raiswell R (1976) The microbiological formation of carbonate concretions in the Upper Lias of N.E. England. *Chem Geol* 18:227–244
- Raiswell R (1988) Evidence for surface reaction-controlled growth of carbonate concretions in shales. *Sedimentology* 35:571–575
- Raiswell R, Fisher QJ (2000) Mudrock-hosted carbonate concretions: a review of growth mechanisms and their influence on chemical and isotopic composition. *J Geol Soc London* 157:239–251
- Schindler PW, Stumm W (1987) The surface chemistry of oxides, hydroxides, and oxide minerals. In: Stumm W (ed) *Aquatic surface chemistry*. Wiley-Interscience, New York, pp 83–110
- Schlanger SO, Jenkyns HC (1976) Cretaceous oceanic anoxic events: causes and consequences. *Geol Mijnbouw* 55:179–184
- Schlanger SO, Arthur MA, Jenkyns HC, Scholle PA (1987) The Cenomanian–Turonian Oceanic Anoxic Event, I. Stratigraphy and distribution of organic carbon-rich beds and the marine $\delta^{13}C$ excursion. In: Brooks J, Fleet AJ (eds) *Marine petroleum source rocks*. Geological Society Special Publication, no 26. Geological Society, London, pp 371–399
- Scopelliti G, Bellanca A, Coccioni R, Luciani V, Neri R, Baudin F, Chiari M, Marcucci M (2004) High-resolution geochemical and biotic records of the Tethyan ‘Bonarelli level’ (OAE2, latest Cenomanian) from the Calabianca-Guidaloca composite section, northwestern Sicily, Italy. *Palaeogeogr Palaeoclimatol Paleoeol* 208:293–317. doi:[10.1016/j.palaeo.2004.03.012](https://doi.org/10.1016/j.palaeo.2004.03.012)
- Scopelliti G, Bellanca A, Neri R, Baudin F, Coccioni R (2006) Comparative high-resolution chemostratigraphy of the Bonarelli Level from the reference Bottaccione section (Umbria–Marche Apennines) and from an equivalent section in NW Sicily: consistent and contrasting responses to the OAE2. *Chem Geol* 228:266–285. doi:[10.1016/j.chemgeo.2005.10.010](https://doi.org/10.1016/j.chemgeo.2005.10.010)
- Scopelliti G, Bellanca A, Erba E, Jenkyns HC, Neri R, Tamagnini P, Luciani V, Masetti D (2008) Cenomanian–Turonian carbonate and organic-carbon isotope records, biostratigraphy and provenance of a key section in NE Sicily, Italy: palaeoceanographic

- and palaeogeographic implications. *Palaeogeogr Palaeoclimatol Paleocool* 265:59–77. doi:[10.1016/j.palaeo.2008.04.022](https://doi.org/10.1016/j.palaeo.2008.04.022)
- Steuber T, Korbar T, Jelaska V, Gušić I (2005) Strontium-isotope stratigraphy of Upper Cretaceous platform carbonates of the island of Brač (Adriatic Sea, Croatia): implications for global correlation of platform evolution and biostratigraphy. *Cretac Res* 26:741–756. doi:[10.1016/j.cretres.2005.04.004](https://doi.org/10.1016/j.cretres.2005.04.004)
- Stumm W (1993) Aquatic colloids as chemical reactants: surface structure and reactivity. *Colloid Surf A* 73:1–18
- Velić I, Vlahović I (eds) (2009) Explanatory notes for the geological map of the Republic of Croatia in 1:300.000 scale. Croatian Geol Institute, Zagreb, p 141
- Velić I, Vlahović I, Matičec D (2002) Depositional sequences and palaeogeography of the Adriatic carbonate platform. *Memorie della Società Geologica Italiana* 57:141–151
- Vlahović I, Tišljarić J, Velić I, Matičec D (2005) Evolution of the Adriatic Carbonate Platform: palaeogeography, main events and depositional dynamics. *Palaeogeogr Palaeoclimatol Paleocool* 220:333–360. doi:[10.1016/j.palaeo.2005.01.011](https://doi.org/10.1016/j.palaeo.2005.01.011)